Phase Segregation Behavior in PE/DOP Blends and Glass-Transition Temperatures of Polyethylene

YEONG-TARNG SHIEH, CHIH-MING LIU

Department of Chemical Engineering, National Yunlin University of Science and Technology, Touliu, Yunlin 640, Taiwan

Received 21 December 2000; accepted 16 March 2001

ABSTRACT: Phase segregation behavior in PEs/DOP blends, interactions between PEs and DOP, and glass-relaxation transitions of PEs were investigated. FTIR, DSC, and TGA data demonstrated that molecular interactions were present between PEs and DOP. DMA data demonstrated that pure PEs each (except HDPE) exhibited two loss maxima at about −20 and −120°C but the PEs/DOP blends (including the HDPE/DOP blend) yielded one new loss maximum at about −60°C. The glass-relaxation transitions corresponding to the three loss maxima on the DMA curves were designated α (−20°C), β (−60°C), and γ (−120°C) transitions and were attributed to the relaxation of the amorphous phases in the interlamellar, interfibrillar, and interspherulitic regions, respectively, based on DMA, WAXD, SAXS, and POM measurements. The controversial T_g values of PEs and their origin were thus clarified in this study. © 2001 John Wiley & Sons, Inc. J Appl Polym Sci 82: 3591–3601, 2001

Key words: polyethylene; phase segregation; interaction; interlamellar; interfibrillar; interspherulite; glass-transition temperature

INTRODUCTION

Dioctyl phthalate (DOP) is usually used as a plasticizer in poly(vinyl chloride) (PVC) processing.[1] DOP may migrate to the surface of the finished PVC products at elevated temperatures and lead to deterioration in mechanical properties because DOP is a low molecular weight compound. To prevent the migration, a high molecular weight plasticizer is sometimes used to substitute completely or partially for the low molecular weight one. Chlorinated polyethylene (CPE) has been reported for this purpose and for improving impact properties of PVC.[2–7] The compatibility between CPE and PVC is dependent on the extent of chlorination of polyethylene and determines the efficacy of plasticization of CPE in PVC. Without chlorination, polyethylene (PE) is believed to be in low compatibility with PVC, because of significant differences in polarity and morphology, and leads to phase separation and thus low plasticization effect of PE on PVC. Paraffin wax, a low molecular weight polyethylene, is often used as a lubricant in PVC processing.[8,9]. Thus, it is important to know the interaction between polyethylene and DOP when these two compounds are used together during PVC processing. There have been no such reports on compatibility or phase segregation behavior in PE/DOP. In this study we set out to investigate the interaction and phase segregation behavior in PE/DOP blends without the presence of PVC.

In molecular composition, PE is a hydrocarbon compound that is considered to have no polarity. DOP has two polar ester linkages that are believed to be not compatible with nonpolar PE.

Correspondence to: Y.-T. Shieh (shiehy@pine.yuntech.edu.tw).

Contract grant sponsor: National Science Council of Republic of China; contract grant number: NSC89-2216-E-224-008.

Journal of Applied Polymer Science, Vol. 82, 3591–3601 (2001)

DOP, on the other hand, has two hydrocarbon tails that are considered compatible with PE due to similar polarity. Each hydrocarbon tail of DOP has a length of 8 carbons and possibly leads to a melt-miscible PE/DOP blend. However, PE is a crystallizable polymer and may involve phase segregation of the amorphous DOP diluent during cooling of the PE/DOP blends. Depending on the distance of segregation, various types of morphology may be created. These segregation types include (1) interlamellar segregation, where segregation of the diluent occurs at the lamellar level, so that the diluent is located in the interlamellar regions; (2) interfibrillar segregation, where the diluent is segregated by a larger distance to the regions between the lamellar bundles in spherulites; and (3) interspherulitic segregation, where the diluent is segregated by the largest distance to the regions between spherulites.[10,11] A blend system does not necessarily exhibit only one type of morphology. Different types of morphology may coexist, thus leading to multiple locations for the amorphous diluent.[12–16]

Segregation of the amorphous DOP diluent in PE is natural, given that the driving force of crystallization of PE tends to separate the diluent. However, how far the diluent is segregated is not well understood. In thermodynamic essence, two entropic forces are developed during the melt-blending of PE/DOP and subsequent cooling of the binary blend. These forces include the following dynamics: (1) during the melt-blending of the binary blend, two constituents tend to incorporate into each other, to reach the highest obtainable entropy; and (2) during cooling of the binary blend from the melt, PE crystallizes and tends to exclude the DOP diluent out of the interlamellar regions.[17] On the other hand, two enthalpic forces are developed in the PE/DOP blend, including (1) the favorable interaction between the hydrocarbon tails of the DOP diluent and the hydrocarbon chains of PE, and (2) the unfavorable interaction between the polar ester linkages of DOP and the nonpolar hydrocarbon PE. The enthalpic force from the favorable interaction and the entropic force, which favors holding the diluent in the interlamellar regions, are against the unfavorable interaction and the entropic force, which favors excluding the diluent out of the interlamellar regions. The distance of segregation of the diluent is consequently dependent on the respective magnitude of the above two enthalpic forces , two entropic forces, the space of the interlamellar regions, and the cooling rate. All of these depend on composition, temperature, and molecular weight.

Depending on the type of segregations, whether interlamellar, interfibrillar, or interspherulitic segregations, the amorphous diluent in each region may exhibit a corresponding glass-relaxation transition. If this is the case, one may clarify the controversial glass-transition temperatures (T_g's) of PE or interpret the origin of these T_g's in a different way. There has been considerable argument as to the position of the relaxation transitions of PE.[1,18–26] The most commonly believed three transitions reported for PE include those termed α, β, and γ relaxation transitions.[18–21] The α-transition occurs just below the melting point and is related to the onset of molecular motion in the crystalline phase. The β-transition occurs at -30 to -20°C and is believed to be associated with the onset of motion at branch points. The peak is absent in completely unbranched PE.[18,21,25] The γ-transition occurs at about -125 to -120°C for both linear and branched PE and is believed to be associated with segmental motion of as few as three or four methylene groups in the carbon–carbon backbone in the amorphous phase, and is considered the primary glass transition of PE.[18,19,21]

In the present report, we set out to investigate the phase segregation behavior in PE/DOP blends and interpret glass-transition temperatures of PE in terms of the distance of segregation of DOP by PE. Influences of molecular weights of LDPE on the phase segregation behavior in LDPE/DOP blends and on the glass-transition temperatures of LDPE were also evaluated. Dynamic mechanical analyzer (DMA), differential scanning calorimetry (DSC), small-angle X-ray scattering (SAXS), wide-angle X-ray diffraction (WAXD), thermogravimetric analyzer (TGA), and Fourier transform infrared (FTIR) were used for this study.

EXPERIMENTAL

Materials and Sample Preparation

All materials were used as received. Polyethylenes used for this study included a high-density polyethylene (HDPE), a linear low-density polyethylene (LLDPE), and three low-density polyethylenes (LDPEs) of differing molecular weights, including LDPE1, LDPE2, and LDPE3. The molecular weights of LDPEs were in the order of

LDPE1 > LDPE2 > LDPE3. HDPE was received from USI Far East Corp. (product number LH606; melt index 1.0 g/10 min; density 0.961 g/cm^3; Taipei, Taiwan). LLDPE was received from ExxonMobil Chemical Company (product number LL3201; 3.5 mol % of 1-hexene comonomer in the copolymer; melt index 0.8 g/10 min; density of 0.925 g/cm^3; Houston, TX). LDPE1 was received from Asia Polymer Corp. (product number H0100; melt index 0.5 g/10 min; density 0.922 g/cm^3; Taipei, Taiwan). LDPE2 was received from Borealis Corp. (product number LE4074; melt index 2.8 g/10 min; density 0.917 g/cm^3; Portugal). LDPE3 was received from Asia Polymer Corp. (product number 7100; melt index 7.3 g/10 min; density 0.917 g/cm^3). Melt indices were determined according to the ASTM D1238 at 190°C and 2.16 kg of loading for all polyethylenes. DOP was supplied by Union Petrochemical Corp. (Taipei, Taiwan). The PE/DOP blends were prepared by mixing PE powder with various amounts of DOP followed by extruding twice in a single-screw extruder (diameter 30 mm; L/D 19; compression ratio 3.5) at 160°C in the feeding zone, 160°C in the compression zone, and 170°C in the metering zone. After extrusions the pelletized sample was compression-molded by a hot press at 150°C for 30 s to make film specimens for instrument measurements.

DMA Measurements

Dynamic mechanical analyzer (DMA 2980; TA Instruments, New Castle, DE) was used to analyze storage moduli, loss moduli, and tan δ of PE/DOP specimens in dimensions of 25 $\times$ 6 $\times$ 0.33 mm (length $\times$ width $\times$ thickness). DMA was measured in the tensile mode at a constant frequency of 50 Hz and a heating rate of 3°C/min from $-$150°C to 100°C.

DSC Measurements

Crystallizations of the blend samples were performed by DSC (DSC 2010; TA Instruments) at a cooling rate of 20°C/min after the samples were heated to 150°C. For thermal fractionation, the samples were heated on the DSC at 10°C/min under nitrogen from 30 to 140°C holding for 10 min, followed by cooling at a rate of 20°C/min to 110°C holding for 30 min, and then the samples were successively cooled by 5°C at 20°C/min. The specimens were maintained at each temperature for 30 min. Thus, the specimens were kept at each of the following temperatures: 110, 105, 100, 95, 90, 85, and 80°C for 30 min and then cooled to 30°C at 20°C/min. The samples were then heated again to 140°C at 10°C/min to obtain the second endotherms, during which several peaks were obtained for each sample.

FTIR Measurements

A Fourier transform infrared spectrometer (FTS 155 FTIR; Bio-Rad, Hercules, CA) with a resolution of 2 cm^{-1} was used to analyze the methylene rocking mode (ρ CH_2) in crystalline polyethylene at 730 and 720 cm^{-1}, arising from a splitting of a single band. The splitting is associated with the crystalline regions of polyethylene and arises from interactions between adjacent molecules in the crystalline phase, which results in both an in-phase and an out-of-phase rocking mode.[27–30]

TGA Measurements

A thermogravimetric analyzer (TGA 2050; TA Instruments) was used to analyze the degradation behavior of specimens under nitrogen at a heating rate of 20°C/min from 30 to 900°C.

WAXD Measurements

Samples for WAXD measurements were prepared by heating the film specimens to 150°C holding for 3 min, followed by cooling at 20°C/min to room temperature. The WAXD measurements were performed at room temperature on a Siemens D5000 X-ray diffractometer (Siemens Medical Systems, South Iselin, NJ) operating at 40 kV and 35 mA using molybdenum radiation with a wave length of 0.7093 Å as an X-ray source. Samples were mounted on a goniometer scanning at 1.2°/min.

SAXS Measurements

Samples for SAXS measurements were prepared by heating the film specimens to 150°C holding for 3 min, followed by cooling to room temperature at 20°C/min. All SAXS measurements were performed at room temperature. The X-ray source was operated at 200 mA and 40 kV and was generated by an 18-kW rotating anode X-ray generator (Rigaku, Japan) with a rotating anode Cu target. The incident X-ray beam was monochromated by a pyrolytic graphite and a set of three pinhole inherent collimators were used so that the smearing effects inherent in slit-collimated small-angle X-ray cameras would be avoided. The

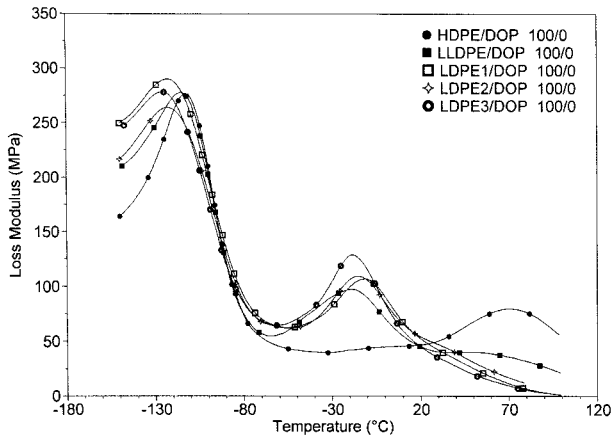

Figure 1 Loss modulus curves of DMA as a function of temperature for various polyethylenes.

sizes of the first and second pinhole were 1.5 and 1.0 mm, respectively, and the size of the guard pinhole before the sample was 2.0 mm. The scattered intensity was detected by a two-dimensional position-sensitive detector (Ordela Model 2201X; Oak Ridge Detector Laboratory) with 256 $\times$ 256 channels (active area 20 $\times$ 20 cm^2 with $\sim$ 1-mm resolution). The sample-to-detector distance was 4000 mm long. The beam stop was around an 18-mm-diameter lead disk. All data were corrected by the background (dark current and empty beam scattering) and the sensitivity of each pixel of the area detector. The area scattering pattern was radially averaged to increase the efficiency of data collection compared with that of a one-dimensional linear detector. Data were acquired and processed on an IBM-compatible personal computer.

Polarized Optical Microscopy

Film samples were prepared by compression in a hot press at 150°C. The films were then heated in a hot stage (FP900; Mettler) under nitrogen to 180°C holding for 5 min and were then cooled at a rate of 10°C/min to 100°C, holding for 24 h for complete crystallizations. The treated samples were then cooled at 10°C/min to 30°C and transferred to a polarized optical microscope (POM; D-07740; Zeiss, Thornwood, NY) to observe their crystal morphologies.

RESULTS AND DISCUSSION

Figure 1 shows loss modulus curves of DMA for various polyethylenes. As can be seen in Figure 1 for pure HDPE, two loss maxima are found at about 70 and -110°C. For LLDPE, three loss maxima are found at about 55, -20, and -115°C. For LDPEs, two loss maxima are found at about -15 and -120°C. Apparently, HDPE and LLDPE exhibit a crystalline relaxation transition at about 70 and 55°C, respectively, but all three LDPEs studied do not show any loss maximum at nearby temperatures. This crystalline relaxation is termed α_c-transition in this study and is attributed to high melting temperature (i.e., high degree of crystallinity, or high density) for HDPE and LLDPE. According to DSC thermograms (not shown in this study) of heating scans at 20°C/min for these polyethylenes, an endotherm for each polymer with a peak temperature is found at 141, 127, and 110°C for HDPE, LLDPE, and LDPEs, respectively. It is thus reasonable that HDPE, having a higher melting temperature, gives a more intense loss maximum than that of LLDPE, which has a lower melting temperature, as shown in Figure 1. The loss maximum at about -20°C is termed α-transition in this study and is present for LLDPE and LDPEs but not for HDPE. The present α-transition was previously reported to be associated with the branching of the polyethylene backbone.[18,19] The finding from Figure 1 is consistent with that in the literature, given that HDPE has a negligible branching, whereas LLDPE and LDPEs exhibit various degrees of branching. The corresponding temperature of the present α-transition to three LDPEs is seen to increase with increasing molecular weight of the polymer. The loss maximum at about -110 to -120°C is termed γ-transition in this study and is present for all polyethylenes studied, among which HDPE exhibits the sharpest loss maximum peak at the highest temperature. All three LDPEs exhibit relatively broad loss maxima peaks at relatively low temperatures compared with those of HDPE and LLDPE. Similar to the α-transitions for three LDPEs, temperatures of the γ-transitions also increase with increasing molecular weights of the polymers.

Figure 2 shows loss modulus curves of DMA for polyethylenes containing 20 phr of DOP. As can be seen in Figure 2, the α_c-transition remains to be seen for the HDPE/DOP (100/20) blend, whereas the α_c-transition becomes negligible for the LLDPE/DOP (100/20) blend. Apparently, DOP is incorporated into LLDPE and interferes with crystallization of LLDPE, resulting in a decrease in the crystalline relaxation transition. The α-transition at about -20°C remains absent

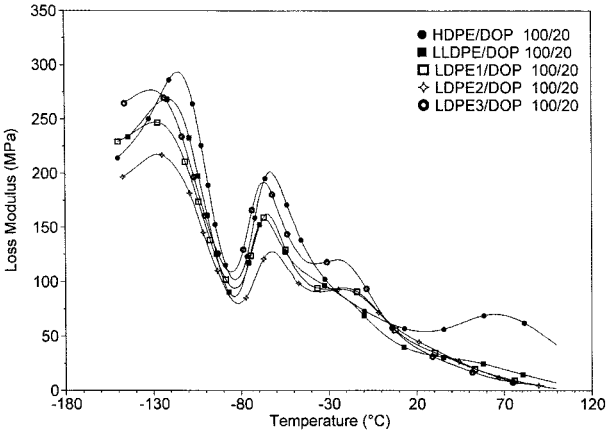

Figure 2 Loss modulus curves of DMA as a function of temperature for various polyethylenes containing 20 phr DOP.

for the HDPE/DOP (100/20) blend. This transition is almost missing for the LLDPE/DOP (100/20) blend and is much decreased in intensity for the LDPEs/DOP (100/20) blends, compared with that of pure polyethylenes. Thus, the α-transition is not simply attributed to the relaxation of the branching as reported in the literature.[18,19] If the present α-transition is purely associated with the branching of polyethylenes, the α-transition of the LLDPE/DOP (100/20) blend should remain to be clearly seen because the branching remains present for LLDPE after addition of DOP. The disappearance of the α-transition of LLDPE upon addition of DOP thus suggests that the interaction between LLDPE and DOP and phase segregation behavior in the LLDPE/DOP blend may affect the α-transition in its intensity and/or its temperature.

The γ-transition at about -110 to -120°C is found for all polyethylenes containing 20 phr DOP. The present γ-transitions are broader in their loss maxima and shift to lower temperatures for all five blends (Fig. 2) than those for pure polyethylenes (Fig. 1). If the γ-transition temperature is considered the primary glass-transition temperature (i.e., T_g), the decreases in T_g's of polyethylenes by the addition of DOP suggest that the plasticization of polyethylenes can be achieved by the addition of DOP. Although the reported origin for this γ-transition, which is associated with segmental motion of as few as three or four methylene groups in the carbon–carbon backbone in the amorphous phase of polyethylenes,[18,19,21] is not in conflict with the finding in this study, the interaction between DOP and polyethylenes and the phase segregation of DOP into various amorphous regions of polyethylenes apparently affect the γ-transition in its intensity and/or its temperature.

New loss maxima at about -60°C are found for all polyethylenes upon addition of 20 phr DOP. These new loss maxima are termed β-transitions because their temperatures are between those of α- and γ-transitions in this study. This new loss maximum for each blend suggests a newly created amorphous region in the corresponding polymer, apparently attributable to the phase segregation of DOP in the polymer. Initially, we suspected this new loss maximum of being attributed to the melting of DOP at nearby temperatures. DSC thermograms (not shown in this study) of heating scans at 20°C/min for polyethylenes/DOP blends, however, do not exhibit any endotherm at nearby temperatures. On the other hand, if the origin of the new loss maximum is really attributed to the melting of DOP at nearby temperatures, the loss maximum peaks of the γ-transitions at about -110 to -120°C should become sharper and shift to higher temperatures for the polyethylenes/DOP blends (Fig. 2) than those for pure polyethylenes (Fig. 1). The γ-transitions, however, are broader in their corresponding loss maxima and shift to lower temperatures for all five polyethylenes containing 20 phr DOP than those for pure polyethylenes. Therefore, the loss maxima at about -60°C should be newly created after addition of DOP into polyethylenes.

Figure 3 shows loss modulus curves of DMA for LDPE2 containing various amounts of DOP. As can be seen in Figure 3 for pure LDPE2, two loss

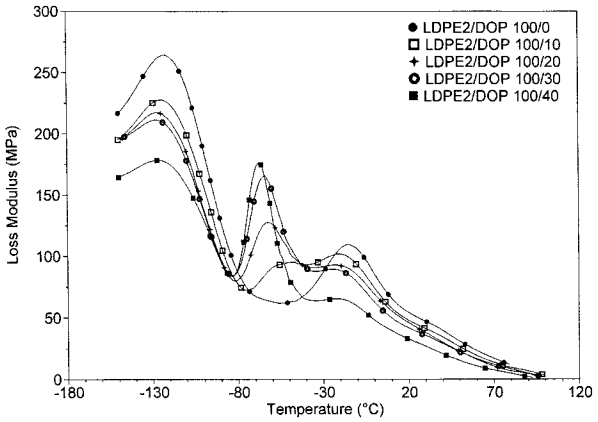

Figure 3 Loss modulus curves of DMA as a function of temperature for LDPE2 containing various amounts of DOP.

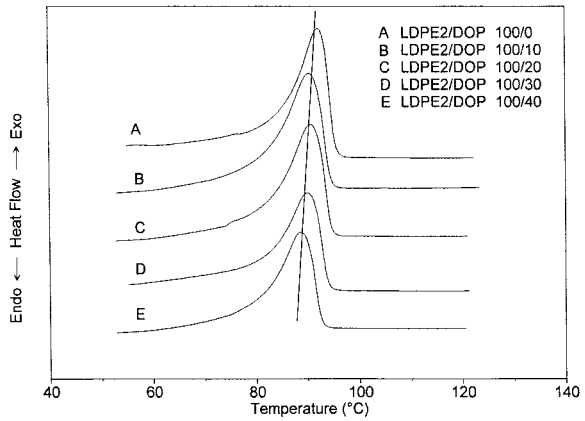

Figure 4 DSC thermograms of cooling scans for LDPE2 containing various amounts of DOP.

maxima corresponding to α- and γ-transitions are present at about -15 and -122°C, respectively. Upon addition of 10 phr DOP, the LDPE2/DOP blend gives a new loss maximum at about -50°C, corresponding to β-transition and two other loss maxima corresponding to α- and γ-transitions shift from about -15 and -122°C for pure LDPE2 to about -24 and -125°C for the blend, respectively. By increasing addition of DOP, temperatures of three loss maxima for the LDPE2/DOP blends are all found to decrease. This suggests that the loss maximum assigned to the β-transition is indeed not attributed to the melting of DOP, the plasticization of LDPE2 is achieved by an addition of DOP, and the plasticization may occur in three amorphous domains. Furthermore, with increasing DOP content, the loss maximum of the β-transition increases in intensity, whereas the loss maxima of both α- and γ-transitions decrease, an indication that the plasticization effect is more significant in an amorphous domain corresponding to the β-transition than that in domains corresponding to α- and γ-transitions.

According to DMA data shown in Figures 1–3 and interpretation and discussion on these data presented above, it is not unreasonable to assign the α-, β-, and γ-transitions to three corresponding amorphous regions. Locations of these amorphous regions and origins of formations of these amorphous regions, however, are not evident at this stage. Based on the description earlier, interactions between polyethylenes and DOP should be present in the binary blends. These interactions may affect crystallization of polyethylenes in the blends upon cooling from the melt-blending. The crystallization of polyethylenes can lead to phase segregation of the amorphous DOP diluent in the blends, resulting in different amorphous locations in the blends, depending on the distance of the phase segregation. In the following, evidence of the interaction and its effect on crystallization of polyethylenes in the blends are demonstrated, followed by investigations of formation and location of the amorphous region in the blends.

The effect of DOP content on the crystallization of LDPE2 is demonstrated by the DSC thermograms of cooling scans, as shown in Figure 4. As can be seen in Figure 4, the crystallization temperature of LDPE2 decreases from 92 to 88°C with increasing DOP content from 0 to 40 phr. As compared with LDPE2, DOP is a low molecular weight molecule and acts as a diluent in the LDPE2/DOP blend. Thus, DOP should help improve the crystallization of LDPE2 if interaction between DOP and LDPE2 is not present. From Figure 4, however, DOP retards the crystallization of LDPE2, suggesting that some sort of interaction is present between DOP and LDPE2. This interaction may involve van der Waals attraction between the hydrocarbon tails of DOP and the hydrocarbon backbone of LDPE2. FTIR spectra, as shown in Figure 5, also provide evidence of a similar effect of the interaction on crystallization of LDPE2. According to the literature,[27–30] the two bands at 730 and 720 cm^{-1}, assigned to the methylene rocking mode (ρ CH_2) in crystalline polyethylene, originate from a splitting of a single band. The splitting is associated with the crystalline regions of polyethylene and

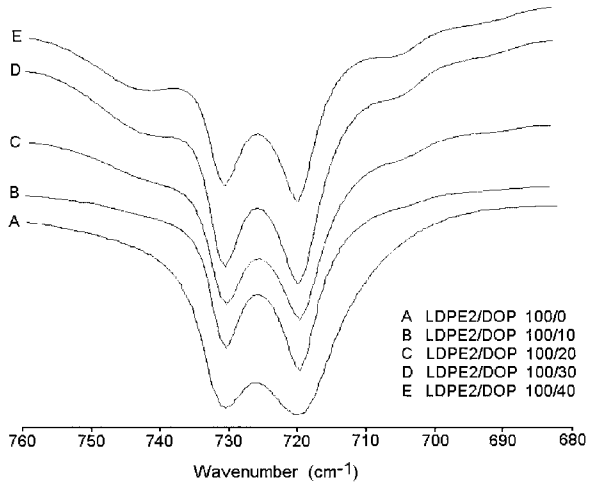

Figure 5 FTIR spectra in the range of 680–760 cm^{-1} for LDPE2 containing various amounts of DOP.

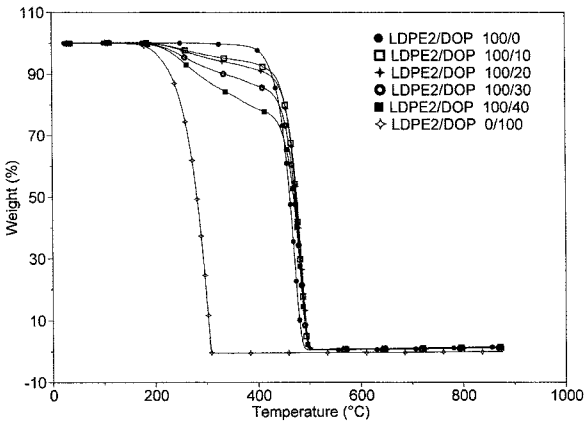

Figure 6 Weight loss curves of TGA as a function of temperature for DOP and the LDPE2/DOP blends containing various amounts of DOP.

arises from interactions between adjacent molecules in the crystalline phase, which results in both an in-phase and an out-of-phase rocking mode.

With increasing crystallization, intensities of the two bands at 730 and 720 cm^{-1} increase at the expense of the broad diffuse characteristic extending from 680 to about 760 cm^{-1}.[29] As can be seen in Figure 5, with increasing DOP content, bands at about 742 and 705 cm^{-1} are found to increase in their intensities, compared to that of bands at 730 and 720 cm^{-1}, an indication that the crystallization of LDPE2 decreases with increasing DOP content. More interaction evidence can be obtained from TGA data, as shown in Figure 6. Without any interaction present between LDPE2 and DOP, the weight loss curve for the LDPE2/DOP blends should involve a two-step weight loss, including the first step that occurs at a lower temperature for the weight loss of DOP and the second step at a higher temperature for that of LDPE2. However, Figure 6 shows a disproportional weight loss to the DOP content in the LDPE2/DOP blends in the heating range from about 200 to about 450°C.

LDPEs are heterogeneous in molecular structure and give multiple melting endotherms after having been thermally fractionated.[31–34] Thermal fractionation was performed on the LDPE2/DOP blends to investigate the effect of the interaction on the crystallization of LDPE2 in the presence of DOP. Figure 7 shows DSC thermograms of heating scans for the LDPE2/DOP blends after thermal fractionation on DSC. As can be seen in Figure 7, multiple endothermic peaks are found for pure LDPE2 and LDPE2/DOP blends. These multiple endothermic peaks correspond to different sizes or perfection of crystals ascribed to structural heterogeneity of LDPE2. The overlapping two peaks for pure LDPE2 with peak temperatures at about 105 and 110°C correspond to the melting of crystals formed from the most structurally regular segments of the LDPE2 molecules. By addition of DOP, the peak at 110°C decreases in intensity with increasing DOP content and completely disappears as the DOP content increases up to 40 phr. This suggests that the crystallization from the most structurally regular segments of the LDPE2 molecules is interrupted by DOP and that DOP is capable of entering into the LDPE crystals.

To investigate whether the incorporated DOP affects the lattice constants (a, b, and c) of LDPE2 crystals, wide-angle X-ray diffraction measurements were performed for the LDPE2/DOP blends, as shown in Figure 8. Because the unit cell of polyethylene is believed to be orthorhombic,[35] the diffraction angles (2θ) at around 9.6, 10.7, 16.2, and 18.0° correspond to the set of planes of (110), (200), (120), and (011), respectively. As can be seen in Figure 8, the diffraction patterns of the blends do not significantly change with the DOP content. By applying the Bragg equation and considering the perpendicular distance between adjacent planes, with indices hkl [$d_{hkl} = (h^2/a^2 + k^2/b^2 + l^2/c^2)^{-1/2}$], lattice constants of the orthorhombic unit cell can be calculated. From these lattice constants, the densities of samples can be determined by considering that there are four CH_2 groups per unit cell.[36] Table I

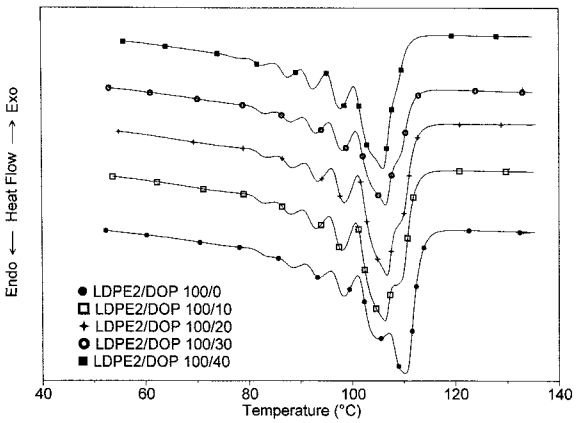

Figure 7 DSC thermograms of heating scans for the LDPE2/DOP blends after thermal fractionation on DSC.

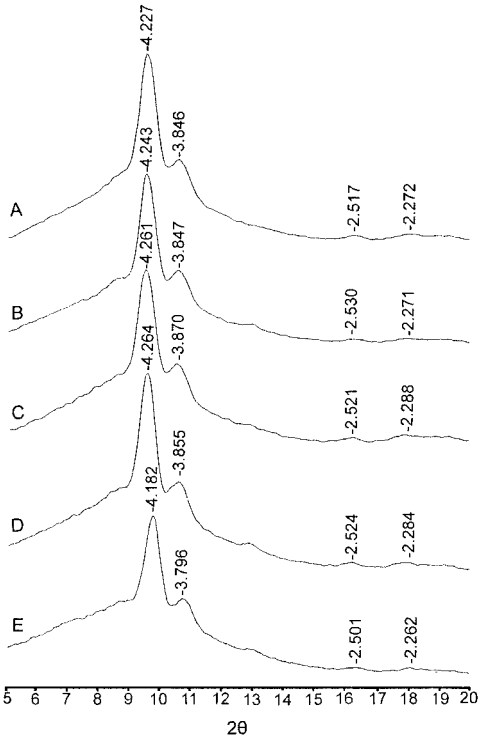

Figure 8 Wide-angle X-ray diffraction patterns for (A) LDPE2/DOP (100/0), (B) LDPE2/DOP (100/10), (C) LDPE2/DOP (100/20), (D) LDPE2/DOP (100/30), and (E) LDPE2/DOP (100/40) blends. The number at the top of a peak denotes the spacing distance of a set of diffraction planes.

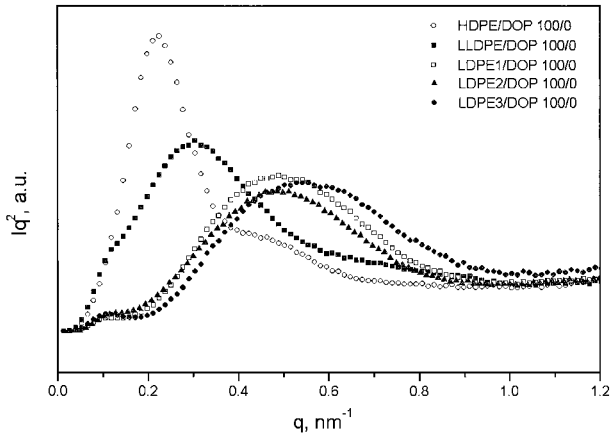

Figure 9 Profiles of Lorentz-corrected intensity (Iq^2) as a function of q for various polyethylenes after cooling treatments at 20°C/min from the melt, where I is the scattering intensity and $q = 4\pi/\lambda \sin(\theta/2)$ (θ = scattering angle).

lists lattice constants of the orthorhombic unit cell and the calculated densities of the unit cell of samples. As can be seen in Table I, with an exception for the LDPE2/DOP (100/40) blend, the lattice constants of LDPE2 crystals in the blends roughly increase with increasing DOP content, an indication that DOP is capable of entering into the location between LDPE2 molecules. The decreasing density of the LDPE2 crystals in the blends with increasing DOP content up to 30 phr also demonstrates that DOP is indeed capable of entering into LDPE2 crystals.

To investigate the distance of the DOP phase segregation by polyethylene crystals, small-angle X-ray scattering measurements were performed for various polyethylenes and their blends with 20 phr DOP. Figures 9 and 10 show the profiles of Lorentz-corrected intensity (Iq^2)[37,38] as a function of q for various polyethylenes and their blends containing 20 phr DOP, respectively, where I is the scattering intensity and $q = 4\pi/\lambda \sin(\theta/2)$ (θ = scattering angle). These samples were prepared by cooling at a rate of 20°C/min from the melt to room temperature at which the small-

Table I Lattice Constants of the Orthorhombic Unit Cell and Calculated Densities of the Unit Cell of LDPE2 Crystals in LDPE2/DOP Blends

Samples	Lattice Constants (Å)			Calculated Density (g/cm^3)
	a	*b*	*c*	
Literature data[a]	7.4	4.93	2.54	1.004
LDPE2/DOP (100/0)	7.692	5.059	2.543	0.940
LDPE2/DOP (100/10)	7.694	5.086	2.538	0.937
LDPE2/DOP (100/20)	7.740	5.104	2.560	0.920
LDPE2/DOP (100/30)	7.710	5.118	2.552	0.924
LDPE2/DOP (100/40)	7.592	5.011	2.535	0.965

[a] Kakudo, M.; Ullman, R. J Polym Sci 1960, 45, 91.

angle X-ray scattering measurements were taken. As can be seen in Figure 9, the q_{max} (i.e., the q value at the maximum Lorentz-corrected intensity) is in the order of HDPE < LLDPE < LDPE1 ≅ LDPE2 < LDPE3. Given that the long period L is equal to $2\pi/q_{max}$, the long periods of these samples can thus be calculated as listed in Table II. The long period is in the order of HDPE > LLDPE > LDPE1 ≅ LDPE2 > LDPE3. Apparently, HDPE exhibits the greatest crystal thickness, followed by LLDPE and by LDPE1 and LDPE2 and by LDPE3. LDPE1 and LDPE2 give greater crystal thickness than that of LDPE3 because of the molecular weight effect on crystallization, with the higher molecular weight for LDPE1 and LDPE2 leading to the greater crystal thickness than that of LDPE3. As can be seen in Figure 10 and Table II, the q_{max} and the calculated long period for the PEs/DOP (100/20) blends are in an order similar to that for PEs. The long periods of HDPE and LLDPE blends exhibit no change, whereas those of LDPEs blends increase upon addition of 20 phr DOP. The increase in the long period is the greatest for the LDPE3 blend, followed by LDPE2 and LDPE1 blends. These increases in the long periods for LDPEs blends suggest that the thicknesses of crystalline lamellae and/or amorphous layer increase. In other words, DOP is able to enter the interlamellar region of LDPEs and leads to an increase in thickness of crystalline lamellae and/or the amorphous layer in the polymers. Thus, Figure 10 indicates that the distance of segregation of the DOP diluent in LDPEs involves the interlamellar segregation.

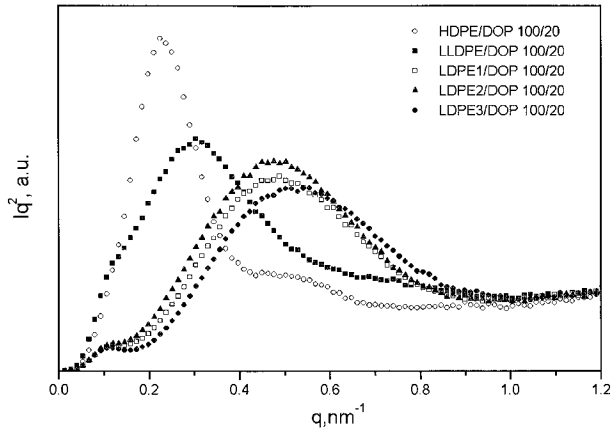

Figure 10 Profiles of Lorentz-corrected intensity (Iq^2) as a function of q for various polyethylene blends containing 20 phr DOP after cooling treatments at 20°C/min from the melt, where I is the scattering intensity and $q = 4\pi/\lambda \sin(\theta/2)$ (θ = scattering angle).

Table II Long Periods of Various Polyethylenes and Their Blends with 20 phr DOP

Samples	Long Period (Å)	Samples	Long Period (Å)
HDPE	282.5	HDPE/DOP (100/20)	282.5
LLDPE	209.4	LLDPE/DOP (100/20)	209.4
LDPE1	130.5	LDPE1/DOP (100/20)	133.1
LDPE2	130.4	LDPE2/DOP (100/20)	133.7
LDPE3	115.5	LDPE3/DOP (100/20)	119.9

Figure 11 shows polarized optical micrographs (POM) for pure LLDPE and the LLDPE/DOP (100/20) blend. Crystal formations can be seen from Figure 11 for both samples. For pure LLDPE, there are many spherulites with a variety of sizes impinging on each other. As can be seen in Figure 11 (micrograph B) for the LLDPE/DOP blend, the spherulites are much decreased in size or are in a much less perfect state, or are even not in the form of spherulites (or perhaps lamellar bundles) dispersing in the amorphous phase. In other words, in addition to the already present interspherulitic segregation, the interfibrillar segregation can be seen in Figure 11 (micrograph B).

Based on wide-angle diffraction, small-angle scattering, and polarized optical microscopy analyses, the interfibrillar segregation is evident after addition of DOP. The newly created loss maxima at about −60°C, as shown in Figures 2 and 3 for various polyethylenes after additions of DOP, can thus evidently be assigned to relaxations of the amorphous phase in the interfibrillar regions. It is not unreasonable to assign the loss maxima at about −20 and about −120°C to relaxations of the amorphous phases in interlamellar and interspherulitic regions, respectively, because the amorphous phase in the interlamellar region can have more steric restriction than that in the interspherulitic region. The controversial T_g values and their origin are thus clarified for polyethylenes. T_g values of polyethylenes from this study should involve those temperatures at about −20°C, −60°C, and −122°C, corresponding to amorphous components in the interlamellar, interfibrillar, and interspherulitic regions, respectively.

CONCLUSIONS

Phase segregation behavior in various polyethylenes/DOP blends and interaction between poly-

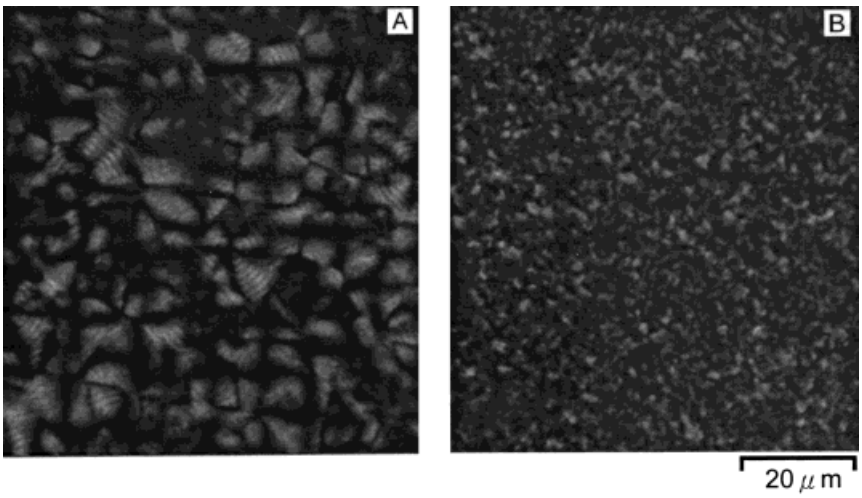

Figure 11 Polarized optical micrographs for (A) pure LLDPE and (B) LLDPE/DOP (100/20) blend.

ethylenes and DOP, and glass-relaxation transitions of polyethylenes were investigated. FTIR, DSC, and TGA data demonstrated that molecular interaction was present between polyethylenes and DOP. The present interaction was developed by the van der Waals attraction between two hydrocarbon tails of DOP and the hydrocarbon backbone of polyethylene molecules and was against exclusion of the DOP diluent out of polyethylene crystals during cooling crystallization from the melt-blending. The distance of segregation of the DOP diluent was governed by the interplay of the enthalpic driving force (i.e., the interaction) and the entropic driving force (i.e., the crystallization). During cooling of the blends from the melt at a rate of 20°C/min, DOP could be segregated into three regions including interlamellar, interfibrillar, and interspherulitic regions based on WAXD, SAXS, and POM data. From DMA data, pure LDPE exhibited two glass-relaxation transitions at about −20 and −122°C but yielded one new glass-relaxation transition at about −60°C after the addition of DOP. These three glass-relaxation transitions, designated α (−20°C), β (−60°C), and γ (−122°C) transitions, were assigned to the amorphous component in interlamellar, interfibrillar, and interspherulitic regions, respectively, based on DMA, WAXD, SAXS, and POM analyses. The controversial T_g values of polyethylenes and their origin were thus clarified and interpreted in a different way in this study.

The authors thank the National Science Council of Republic of China for financial support for this work under contract number NSC89-2216-E-224-008. They are also grateful to Prof. Tsang-Lang Lin and Dr. Wen-Jun Liu of the Department of Engineering and System Science and Prof. Hsin-Lung Chen of the Department of Chemical Engineering at National Tsing-Hua University for their assistance in SAXS measurements and valuable discussions.

REFERENCES

1. Mark, H. Encyclopedia of Polymer Science and Engineering, 2nd ed., Vol. 17; Wiley: New York, 1989.
2. Brydson, J. A. Plastics Materials, 6th ed.; Butterworth-Heinemann: Oxford, 1995.
3. Xu, X.; Meng, X.; Chen, K. Polym Eng Sci 1986, 27, 391.
4. Yang, W.; Wu, Q.; Zhou, L.; Wang, S. J Appl Polym Sci 1997, 66, 1455.
5. Gerlach, D. Kunststoffe Plast Eur 1998, 88, 47.
6. Tse, A.; Laakso, R.; Baer, E.; Hiltner, A. J Appl Polym Sci 1991, 42, 1205.
7. Chen, C. H.; Wesson, R. D.; Collier, J. R.; Lo, Y. W. J Appl Polym Sci 1995, 58, 1087.
8. Mondragon, M.; Flores, A. C. J Vinyl Technol 1993, 15, 46.
9. Falter, J. A.; Geick, K. S. J Vinyl Technol 1994, 16, 112.
10. Stein, R. S.; Khambatta, F. B.; Warner, F. P.; Russell, T.; Escala, A.; Balizer, E. J Polym Symp 1978, 63, 313.
11. Chen, H. L.; Li, L. J.; Lin, T. L. Macromolecules 1998, 31, 2255.
12. Defieuw, G.; Groeninckx, G.; Reynaers, H. Polym Commun 1989, 30, 267.
13. Defieuw, G.; Groeninckx, G.; Reynaers, H. Polymer 1989, 30, 595.

14. Hudson, S. D.; Davis, D. D.; Lovinger, A. J. Macromolecules 1992, 25, 1759.
15. Huo, P. P.; Cebe, P.; Capel, M. Macromolecules 1993, 26, 4275.
16. Sauer, B. B.; Hsiao, B. S. J Polym Sci Polym Phys Ed 1993, 31, 901.
17. Russell, T. P.; Ito, H.; Wignall, G. D. Macromolecules 1988, 21, 1703.
18. Kline, D. E.; Sauer, J. A.; Woodward, A. E. J Polym Sci 1956, 22, 455.
19. Reding, F. P.; Faucher, J. A.; Whitman, R. D. J Polym Sci 1962, 57, 483.
20. McKenna, L. W.; Kajiyama, T.; MacKnight, W. J. Macromolecules 1969, 2, 58.
21. Stehling, F. C.; Mandelkern, L. Macromolecules 1970, 3, 242.
22. Davis, G. T.; Eby, R. K. J Appl Phys 1973, 44, 4274.
23. Boyer, R. F. Macromolecules 1973, 6, 288.
24. Wedgewood, A. R. Ph.D. Dissertation, University of Washington, Seattle, 1982; University Microfilms International, Ann Arbor, MI,1984; pp. 246–248.
25. Moore, R. S.; Matsuoka, S. J Polym Sci Part C 1964, 5, 163.
26. Boyer, R. F. J Polym Sci Part C 1966, 14, 3.
27. Krimm, S.; Liang, C. Y.; Stutherland, G. B. J Chem Phys 1956, 25, 549.
28. Koenig, J. L.; Tabb, D. L. J Macromol Sci Phys Part B 1974, 9, 141.
29. Hendra, P. J.; Jobic, H. P.; Holland–Moritz, K. J Polym Sci Polym Lett Ed 1975, 13, 365.
30. Tashiro, K.; Stein, R. S.; Hsu, S. L. Macromolecules 1992, 25, 1801.
31. Adisson, E.; Ribeiro, M.; Deffieux, A.; Fontanille, M. Polymer 1992, 33, 4337.
32. Keating, M. Y.; McCord, E. F. Thermochim Acta 1994, 243, 129.
33. Wolf, B.; Kenig, S.; Klopstock, J.; Miltz, J. J Appl Polym Sci 1996, 62, 1339.
34. Shieh, Y. T.; Chen, J. S.; Lin, C. C. J Appl Polym Sci 2001, 81, 591.
35. Kakudo, M.; Ullman, R. J Polym Sci 1960, 45, 91.
36. Sperling, L. H. Introduction to Physical Polymer Science, 2nd ed.; Wiley: New York, 1992.
37. Seymour, R. B.; Carraher, C. E. Polymer Chemistry; Marcel Dekker: New York, 1988.
38. Koberstein, J. T.; Galambos, A. F. Macromolecules 1992, 25, 5618.